ARTICLE OPEN

Check for updates

Strain-enhanced electrical performance in stretchable semiconducting polymers

Qing Zhou[1], Zhihui Wang[1], Yongkun Yan[1], Longfei Yang[1], Kai Chi[1], Yangjiang Wu[1], Wenhao Li[1], Zhiying Yi[1], Yunqi Liu[1] and Yan Zhao[1]✉

Intrinsically stretchable semiconducting polymers are promising candidates for developing wearable electronics, but remain underdeveloped because the correlation between the microstructural evolution during stretching and the resultant charge transport is not clearly understood. In this study, we clarify the impact of molecular orientation on the dynamic performance of stretched semiconducting polymers, controlling molecular orientations via solvent-dependent spin-coating. We found that strain-enhanced electrical performance is feasible by quelling disorders within the face-on-packed aggregates. Strain facilitates 3D ordering in face-on-packed films, but increase the π-π orientation disorders and lamellar dislocation in the edge-on analogue, which contribute inversely to the charge transport. Consequently, the face-on samples maintain strain-resistant energetic disorder and a 1.5× increase in on-current, achieving a 10-times-higher retention than the edge-on analogue upon 100% strain. Furthermore, we developed a reliable way for measuring the photoelectrical stretchability of semiconducting polymer. This study contributes to developing high-performance stretchable semiconducting polymers.

npj Flexible Electronics (2023)7:35 ; https://doi.org/10.1038/s41528-023-00269-w

INTRODUCTION

Intrinsically stretchable organic field-effect transistors (OFETs) based on conjugated polymers are attracting intensive attention for their potential applications in wearable, intelligent and biomimicking electronics with the merits of lightweight, cost-effectiveness, and processability on large scales[1–10]. However, developing semiconducting polymers with excellent mechanical and electrical performances remains challenging, especially for n-type organic semiconductors[11–14], because the underlying correlation between their microstructure and charge transport under strain is poorly understood. Most organic transistors experienced declining electrical performance upon stretching, owing to multiscale strain-induced morphological damages, which significantly impede efficient charge transport[15–18]. Therefore, it is challenging but vital to design and process polymer semiconductors with strain-resistant performance.

Understanding the interplay between morphological evolution and its resultant charge carrier mobility during stretching is key to design semiconducting polymers with high mobility and stretchability. From the viewpoint of molecule structure, π-conjugated backbone units and linearly extended chains with folding and entangling structure enable polymer semiconductors with potentially high mobility and inherent stretchability. Efficient charge transport can be achieved by precisely tuning the film morphology and molecular orientation[19–21]. In particular, an edge-on packing structure with π-π conjugated units parallel to the channel is favored for most semiconducting polymers to construct laterally structured OFETs with high mobility[22–24], whereas the face-on packing structure is preferred in the organic photovoltaic devices with a vertical charge transport path[25–28]. To achieve high stretchability, recent advancements in stretchable organic field transistors recommended researchers the following noteworthy schemes based on the understanding of correlation between structure and performance under stain: (1) tailoring backbone and side chains with nonconjugated units to increase the chain flexibility by weakening rigidity;[29–31] (2) introducing dynamic bonds to dissipate strain energy through reversible bonding, for example, H-bonding and metal–ligand coordination;[32–35] (3) elastomer blending to dissipate strain energy through elastomer extension;[36,37] and (4) using small-molecule additives to increase the free volume for polymer chain dynamics[3,38]. In summary, reversible molecular interactions, lower crystallinity and loosely molecule packing are proved to be the mainly structural origins of stretchability in conjugated polymer films. Aside from the aforementioned structural factors ranging from a molecule scale to film morphology level, the impact of the orientation of conjugated polymer backbones on the dynamic performance of semiconducting polymers has rarely been investigated, limited by the access to easily-modulated molecular packing orientation and dynamic morphology characterization.

In this study, we demonstrate the evident impact of orientation of conjugated backbones on morphological evolution and electrical performance of stretchable organic semiconductors. N2200 was selected as a model compound because of its representative semi-crystalline structure of polymer semiconductors and easily modifiable packing structures, as well as relatively high mobility. Combining investigation on electrical performance and detailed morphological characterizations through GIWAXS and ultraviolet diffuse scattering (UV-DRS), we revealed that robust electrical performance under large strain can be realized by quelling the microstructure disorders within the face-on packed aggregates. Strain facilitated the spatial packing ordering of face-on aggregates, while increased the structural disorder in edge-on-packed films, which originated from the rotation of crystalline domains to realize face-on orientation. Owing to the promoted spatial packing ordering in face-on packing films, a more efficient charge transport with high on-current retention of 150% was achieved under the strain of 30%, yielding a nearly 2× increase in mobility, which was considerably higher than that in the edge-on-packed films. Such strain-enhanced electrical performance in

[1]Laboratory of Molecular Materials and Devices, Department of Materials Science, Fudan University, 200433 Shanghai, P.R. China. ✉email: zhaoy@fudan.edu.cn

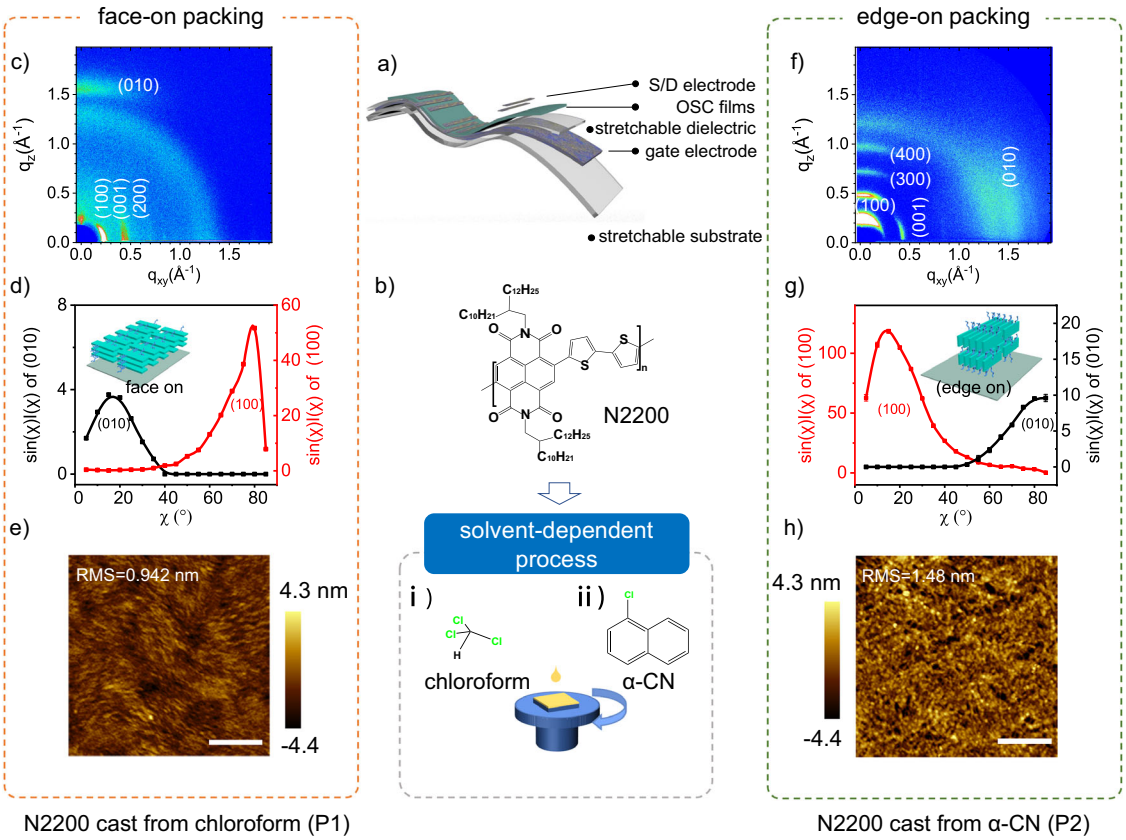

Fig. 1 Illustrations and results of tuning the molecular orientation of N2200-polymer-based films. a Schematic of stretchable organic transistors, where S/D represent source and drain electrodes and OSC represents organic semiconductor, respectively. **b** Tuning the molecular orientation of N2200-based films via solvent-dependent spin-coating. **c**, **d**, **f**, **g** 2D GIWAXS patterns of spin-coated films P1 and P2, and the corresponding (100) and (010) pole figures (see detailed calculations in Supplementary Fig. 3). **e**, **h** AFM images of P1 and P2. All the semiconducting polymer films we used were annealed at 120 °C for 30 min after spin-coating process. The RMS of both films are values of an area of 2 μm*2 μm. Scale bar, 500 nm.

unmodified semiconducting polymer films is rarely reported. Based on the pristine face-on-packed N2200 films, an organic inverter with stable performance up to 100% strain was fabricated, with a recording gain of 65. Our results demonstrate that a more stable electrical performance is accessible by controlling the packing orientation of polymer chains in a face-on packing structure in stretched semiconducting films.

RESULTS AND DISCUSSION

Molecule-orientation-dependent electrical performance in stretchable OFETs

To investigate the impact of molecular orientation on the electrical performance of stretched semiconducting polymer films, N2200 was fabricated using a spin-coating method with different solvents to control the molecular packing structure (Fig. 1). As far as we know, the molecular orientation of polymer semiconductors can be manipulated by controlling the solution aggregation and film drying time: on the one hand, degree of aggregation can be modulated by the solvent molecule volume, where larger molar volume impedes high degree of polymer chain aggregations because of the strong steric hindrance; on the other hand, high boiling point of solvent helps to realize a more stable packing structure of the polymer films. Thus, we dissolved N2200 in chloroform and chloronaphthalene (α-CN), which demonstrate significantly different molar volumes and boiling points to each other, to obtain face-on–dominated and edge-on–dominated packed N2200 films on octadecyltrichlorosilane (OTS)–modified Si/SiO_2 substrates, respectively[39]. The prepared films were applied to GIWAXS characterization to confirm the expected orientations. The N2200 film cast from chloroform (denoted as P1) exhibited a typical face-on packing orientation (Fig. 1c), with (h00) peaks (lamellar packing) appearing in the in-plane direction and the anticipated π-π stacking signal (010) appearing in the out-of-plane direction near $q_z = 1.6\ Å^{-1}$, whereas the α-CN-cast N2200 film (denoted as P2) exhibited an edge-on-dominated packing orientation (Fig. 1f). The corresponding pole figures constructed using the (010) and (100) peaks revealed the preferred packing structures of both films (Fig. 1d, g, and S1), too[40,41]. Note that, films cast on the silicon wafer without OTS modification demonstrate the same molecular orientation as films cast on the OTS modified silicon wafer (Supplementary Fig. 2). Despite being cast from different solvents, both films showed homogenous morphologies, with similar roughness values (root-mean-square [RMS] roughness for P1 and P2: 0.942 and 1.48 nm, respectively) and no visible phase separation, as confirmed by atomic force microscopy (AFM; Fig. 1e, h). To evaluate the stretchability of P1 and P2, a film-on stretching measurement was performed under an optical microscope. The equivalent crack onset strain (COS) suggested that a similar stretchability of both films (Supplementary Fig. 4), owing to the same molecular structure and semicrystalline nature of the investigated polymer films (COSs of P1 and P2: 30% and 35%, respectively). These results indicate that the molecular orientation of the N2200 films was precisely

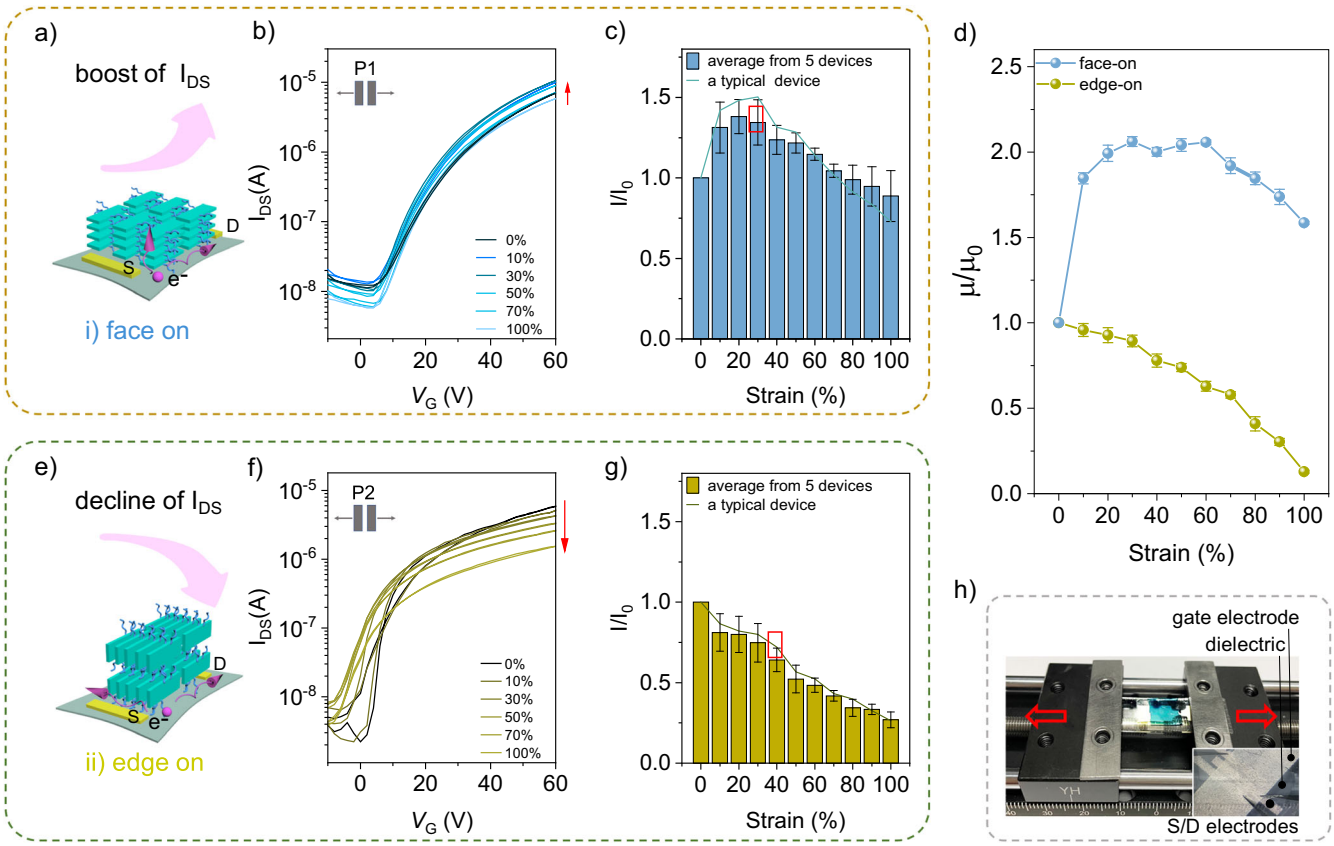

Fig. 2 Molecule-orientation-dependent electrical performance of stretchable OFETs. a, **e** Schematics of charge transport in face-on/edge-on aggregates. S and D represent the source and drain electrodes, respectively. **b**, **f** Transfer curves of P1- and P2-based stretchable OFETs with channel length parallel to the strain. **c**, **g** Ratio of on-current in devices under strain to that in their initial state (red boxes indicate crack onset strains of P1 and P2). Error bars represent standard deviation of 5 individual devices. **d** Ratio of mobilities of stretched and pristine OFETs. The mobility data were extracted with the consideration of the geometric changes of the devices and the varying capacitance of stretched dielectric layer (Supplementary Tables 1, 5). Error bars represent standard deviation of saturation mobilities calculated for 3 times from 1 transfer curve. **h** Optical images of the stretchable OFETs.

controlled using a solvent-dependent spin-coating method. These films were subsequently used as active layers in stretchable organic field-effect transistors.

To evaluate the electrical properties of the prepared films with different packing structures, fully stretchable OFETs with a bottom-gate, top-contact structure were fabricated by a completely soft-lamination method (Fig. 1a, Supporting information). Transfer and output tests were performed by gradually increasing the strain from 0% to 100% at 10% steps on a device in the glove box (Fig. 2h). All the fully stretchable OFETs exhibited stable electrical performance at the initial state, as shown by the typical output and transfer curves in Supplementary Fig. 6. All the detailed performance parameters were summarized in Supplementary Table 2. A mobility of 0.105 $cm^2 V^{-1} s^{-1}$ was obtained for the stretchable OFETs based on the face-on-packed P1 film, along with a threshold voltage (V_{th}) of 4.4 V and negligible hysteresis (Supplementary Fig. 6, Supplementary Table 2). These stretchable OFETs exhibited rational electrical performance compared to their counterparts fabricated on a Si/SiO_2 substrate (Supplementary Figs. 7, 8), considering the low dielectric constant of the stretchable styrene-ethylene-butylene-styrene (SEBS) dielectric layer (Supplementary Fig. 8).

The fully stretchable transistor based on N2200 films with different packing orientations shows different electrical performance as a response to the strain (Fig. 2). In conjugated polymer films, charge transport occurs along the polymer backbones as well as π-conjugation inter-chains. Essentially, for OFETs with a lateral structure, charge transport demonstrates different spatial distribution in a single crystalline domain because the different orientations of polymer backbones (Fig. 2a, e). For the stretchable OFETs based on face-on-packed N2200 film, the on-current in the parallel direction increased continuously with the strain (prior to COS), achieving a high retention of 150% prior to the COS (at 30% strain; Fig. 2b). This unexpected increase in the on-current under strain for pristine semiconducting polymer films has rarely been reported. Upon stretching to 30%, the organic transistor exhibited a mobility of 0.223 $cm^2 V^{-1} s^{-1}$, which was two times that of the unstrained specimen, and remained stable until 100% strain (Supplementary Table 2). In contrast, both the on-current and mobility experienced a monotonic drop when increasing strain was applied to the edge-on-packed N2200 film (Fig. 2d, f, g). Only one-fourth of the on-current remained after stretching to 100%. Essentially, the face-on sample exhibited a ten-times-higher retention of mobility than that of the edge-on-packed film in the twofold-stretched OFETs (Supplementary Table 2). Similarly, for the direction perpendicular to the strain, OFETs based on the face-on packed films also demonstrate a more promising performance than the edge-on cases (Supplementary Figs. 10, 11). This molecular-orientation-dependent electrical performance of stretchable OFETs has rarely been studied, particularly the strain-induced increase in the on-current of face-on-packed films.

Strain-induced morphological evolution

To elucidate the structural origin of the molecule-orientation-dependent electrical performance in aforementioned stretchable

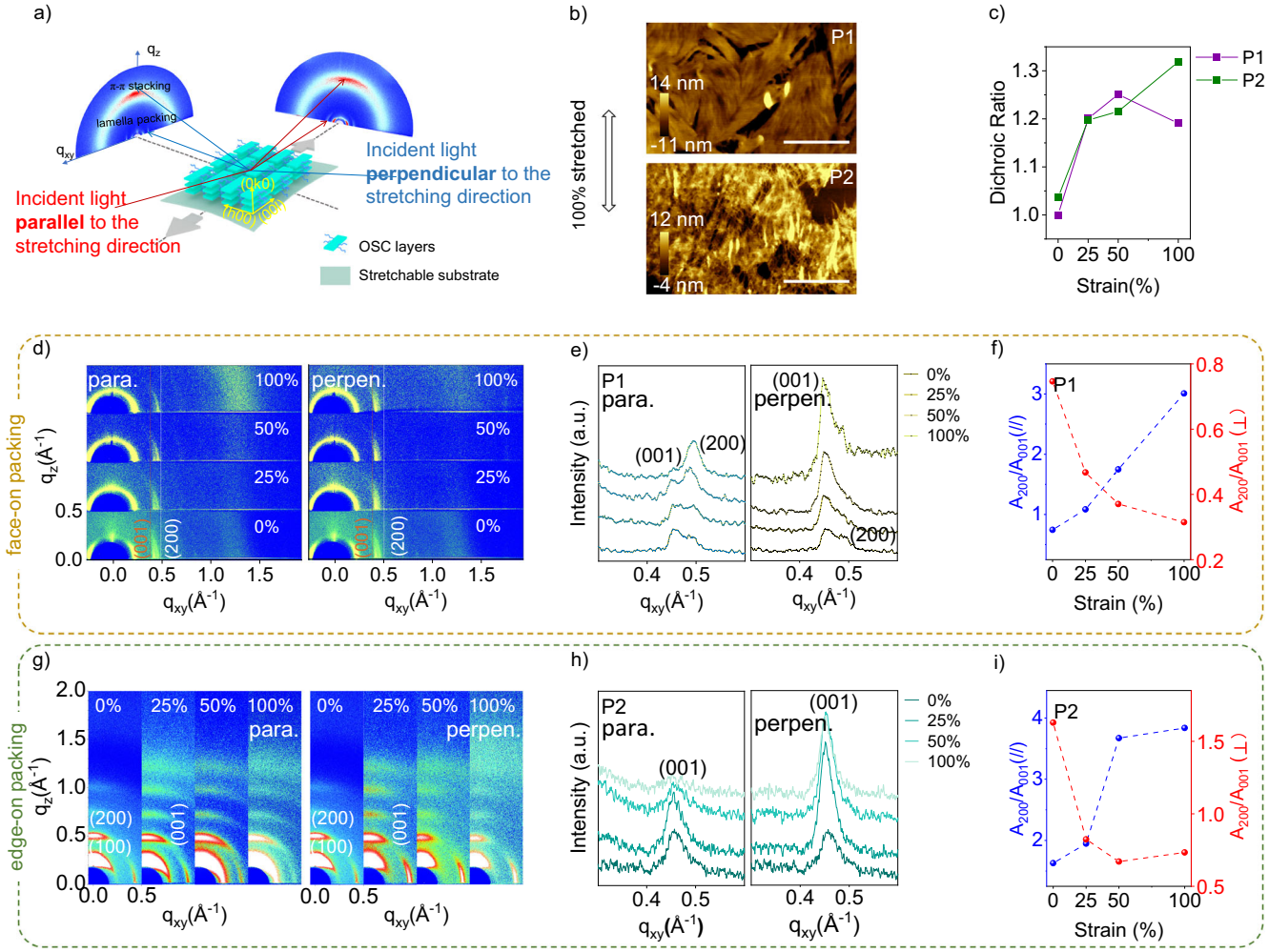

Fig. 3 Strain-induced alignment of aggregates in conjugated polymer films. a Schematic illustrating Grazing-Incidence Wide-Angle X-ray Scattering (GIWAXS) analysis of the stretched semiconductors. **b** AFM images of stretched P1 and P2 films (roughness values of P1 and P2: 1.17 and 1.61 nm, respectively). The RMS of both films are averaged values of 5 randomly selected area (avoiding cracks) of 0.25 μm*0.25 μm in the AFM images of targeted films. Scale bar, 500 nm. **c** Dichroic ratio of 0-0 peak with the light parallel and perpendicular to the stretching direction in P1 and P2 films. **d**, **g** GIWAXS patterns of P1 and P2, and (**e**, **h**) the corresponding profiles obtained under strain using incident light oriented parallel and perpendicular to the stretching direction. The I-q curves are sliced in the region $\chi = 79–81°$ (**f**, **i**) the ratio of peak intensity A_{200}/A_{001} determined using incident light parallel and perpendicular to the stretching direction for the P1 and P2 films.

OFETs, AFM, polarized ultraviolet spectroscope, GIWAXS, and UV-DRS were performed. In all the characterization experiments, the conjugated polymer films were stretched to various strains on a polydimethylsiloxane (PDMS) stretchable substrate and pasted back onto a rigid substrate.

The strain-induced polymer chain alignment in the substrate plane has been continually reported recently, and is thought to significantly influence the electrical performance of organic semiconductors. AFM was performed on the investigated films before and after stretched to study the film morphology. The aggregates in the pristine films demonstrate a homogeneous and isotropic topography (Fig. 1e, h), while after being stretched to 100% strain, both films showed an aligned texture along the tensile direction (Fig. 3b, Supplementary Fig. 12). This polymer chains alignment is in good agreement with the results of polarized UV-vis spectroscopy, in which the intensities of the 0-0 peaks (~701 nm) parallel and perpendicular to the stretching show a remarkable anisotropy upon strain in both films (Fig. 3c, Supplementary Fig. 13). Subsequently, Dichroic ratios as high as 1.31 (P1) and 1.24 (P2) are obtained when stretched to 100% strain. The strain-induced chains alignment is obviously affected by the mechanical stretchability of polymer films. After cracks generation, films adjacent to the cracks get released. Meanwhile, films away the cracks are still under tensional state to maintain more energy for further cracks propagation. The stress distribution near the crack tip were previously visualized via experimental measured winkles and the finite element simulations by Gu's group[42]. With the density and size of the cracks increase further, strain energy maintained in the tensional region releases and polymer chains get released and less aligned (Fig. 3c, i). Given that the polymer films are mechanical stretchable enough, e.g., some previously reported DPP films show no macrocracks over entire investigating range, polymer chains are supposed to be more orientated under continuous strain[34]. All these results confirm that conjugated polymer chains were aligned to the stretching direction under strain.

Aside from the polymer chain motion, the morphological evolution of crystalline regions in semiconductor films has been paid more attention, as the charge transport occurs mainly in these ordered regions. The stretched films were applied to ex-situ GIWAXS analysis to gain insight into the morphological evolution of the crystalline regions under strain (Fig. 3a). Note that, in order

to apply a quantitative analysis on the signals, the samples were carefully prepared to minimize volume deviation (supporting information, Supplementary Fig. 14). In semicrystalline polymer films, the lamellar packing, and polymer chains are orthogonal to each other, represented as (h00) and (00 l) peaks in the 2D GIWAXS patterns, respectively (Fig. 3d, g). When the crystalline region demonstrates preferred alignment in plane, the (h00) and (00 l) signals result in an anisotropic distribution as incident light parallel and perpendicular to the oriented direction. Here, for the face-on packing N2200 films, the (200) peaks (marked with a white line) get stronger as the strain increases in the parallel direction, and decline in the perpendicular direction. On the contrary, the (001) peaks experience an inverse change for corresponding cases. A line cut from $q_{xy} = 0.3–0.6\ Å^{-1}$ show the intensity distribution of (200) and (001) peaks clearly (Fig. 3e). The continuous and inverse trends of (200) and (001) peak intensity upon increasing strain are attributed to the crystallites alignment under strain. To demonstrate this strain-induced in-plane chains alignment more clearly, ratios of peak intensity of (200) to (001) at each illumination are extracted as a function of strain (Fig. 3f, i). As shown in Fig. 3f, for the incident light parallel to the strain, intensity ratio of A_{200}/A_{001} demonstrates linear increasing upon strain and reaches up to 3 as two folds stretched. As polymer chains orientate along the strain direction, higher portion of lamella packing contributes the increased (200) signal, while the conjugated backbones become less "detectable" with the long axis orientated the incident direction. A similar trend of the peak intensities is observed in the edge-on-packed films (P2), too (Fig. 3h, i, Supplementary Fig. 14). All these results suggest that, for both films, crystalline region in the conjugated polymer films was aligned along the tensile direction. That means an ordered crystalline structure was achieved in the substrate plane. Note that, the slight decline of the anisotropy in P2 at 100% strain is likely due to the crack propagation (Supplementary Fig. 4, Fig. 3i). Furthermore, both films demonstrate a higher value of anisotropic ratio calculated from GIWAXS than that from UV-vis polarized spectra scope (Supplementary Fig. 13), indicating the more oriented alignment of crystalline region than the amorphous region.

The GIWAXS results were comprehensively analyzed to investigate the dynamic π-π stacking orientation under strain. Owning to the polymer chains folding and intertwining nature[43], efficient charge transport within the semiconducting polymer films relies on the π-π conjugated interaction between adjacent chains, which demands for highly oriented π-π stacking in the aggregation scale[18,21,44]. The π-π orientation in the face-on- and edge-on-packed N2200 films under varying strain was investigated by extracting the (010) peak intensity as a function of the azimuth angle (χ). As demonstrated in Fig. 4a, b, for the face-on packed N2200 polymer films, the (010) peaks show strain-insensitive azimuth distribution in the direction parallel to the strain; in the direction perpendicular to the strain, (010) peaks exhibit a shrinking azimuth angle distribution upon stretching, with the peak intensity near $\chi = 90°$ showing a remarkable increase. In aligned conjugated polymer films, π-π stacking peaks appear only in the out-of-plane direction when the incident light is perpendicular to the chains[13]. Hence, the sharp increase of (010) peak near $\chi = 90°$ in the perpendicular direction indicates that the aligned polymer backbones achieve more orientated π-π stacking. This strain-promoted packing ordering can be interpreted by the crystallite rotation in stretched polymer films, in which the domains get dragged to be more parallel to the substrate, partially dissipating the strain energy[31,44]. In contrast, for edge-on-packed N2200 films, such crystalline rotation leads to π-π stacking disorder of polymer backbones, as confirmed by the widening azimuth distribution of (010) peaks in both directions upon strain (Fig. 4d, e). Because of the azimuth-angle-dependent intensity distribution of GIWAXS, the (010) signal in the out-of-plane direction for edge-on packing conjugated films are too blurry to be clearly recognized. Hence, we calculated the relative population of the face-on/edge-on aggregates in the edge-on-packed conjugated polymer films to confirm the strain-induced crystal rotation, following a procedure we mentioned above (Supplementary Fig. 15, Supplementary Fig. 3).When applied to increasing strain, the edge-on-packed conjugated polymer films demonstrate a high portion of more face-on aggregates ($\chi < 60°$) as regards to the initial films[20]. These results verified that crystalline domains take a rotation to a more face-on orientation to dissipate the strain energy. However, such rotation rises the π-π stacking disorder vastly in the edge-on-packed films.

We assume that the different behaviors of aggregates are results of the different spatial geometry of face-on and edge-on packed aggregates. As reported previously, conjugated polymer chains tend to assume a lamellar crystalline form when cast into films, in which the face-to-face contact between conjugated backbones was limited within tens of angstrom (~0.39 Å), whereas along the long axis of backbones crystalline, the crystalline structure extends to 2–3 nm, and the lamellar packing tends to be the longest with a length of 4–5 nm (Fig. 4e, f)[45]. When applied tension parallel to the substrate, the lamellar crystals tend to confront to the tension with the narrowest facet to minimize the torque for achieving a metastable state. For the edge-on packing structure, lamellae are prone to rotate upon tension because of a large torque generated from the large facet perpendicular to the tension. This morphology evolution can be well interpreted by the non-equivalent change of intensity ratio (A_{200}/A_{001}) in P2 under the strain of 25% (prior to COS). The small increment of A_{200}/A_{001} along the stretching is only attributed to the in-plane alignment, while the large reduction of that ratio perpendicular to the stretching is a mutual result of the in-plane alignment and out-of-plane crystallites rotation. In contrast, the face-on-packed lamellae exhibit high stability under strain thanks to the initial minimal facet against the tension.

The strain-induced rotation of the aggregates has rarely been reported[31,46], however, polymer chains have been found to exhibit a bimodal packing structure in those studies, thereby hindering efforts into distinguishing the impact of the molecular packing orientation on the dynamic electrical performance and morphological evolution. Herein, our results provide an evident witness of the crystalline domains rotation to dissipate the strain energy in both sorts of unimodal packing films. Through the alignment of the crystalline domains in plane and reorientation of the π-π stacking out of plane, a strain-induced 3D ordering in face-on aggregates is achieved.

A further exhaustive analysis into the lamellae packing distance reveals that aggregates with different packing structures experienced different molecule packing behaviors under strain. The lamellar packing- and π-π stacking distance of P1 and P2 under strain are summarized in Supplementary Table 3. As shown in Fig. 4g, the (100) peaks in face-on aggregates retain their shape and center as strain increase from 0% to 100%, which means the adjacent polymer chains remain in equivalent ordering without dislocation as regard to the initial films. However, in the edge-on packed films, a remarkable shift of (100) peak to the low q_{xy} occurs, indicating an expansion of d-spacing between the lamellar layers (from 22.66 Å to 24.03 Å, Fig. 4i, j, Supplementary Table 3). This wider d-spacing, likely resulted from a lower ordering along the side chain direction or a lower degree of side chain interdigitation[40,44], provides more space for fluctuation of backbones and side chains, which directly gives rise to the backbone disorder and impedes efficient charge transport. The orientation-dependent lamellae distance proves that molecule packing structure have a significant impact on the lamellae packing ordering in stretched semiconducting polymer films.

These results confirmed the different behaviors of the face-on/edge-on aggregates during the strain energy dissipation process.

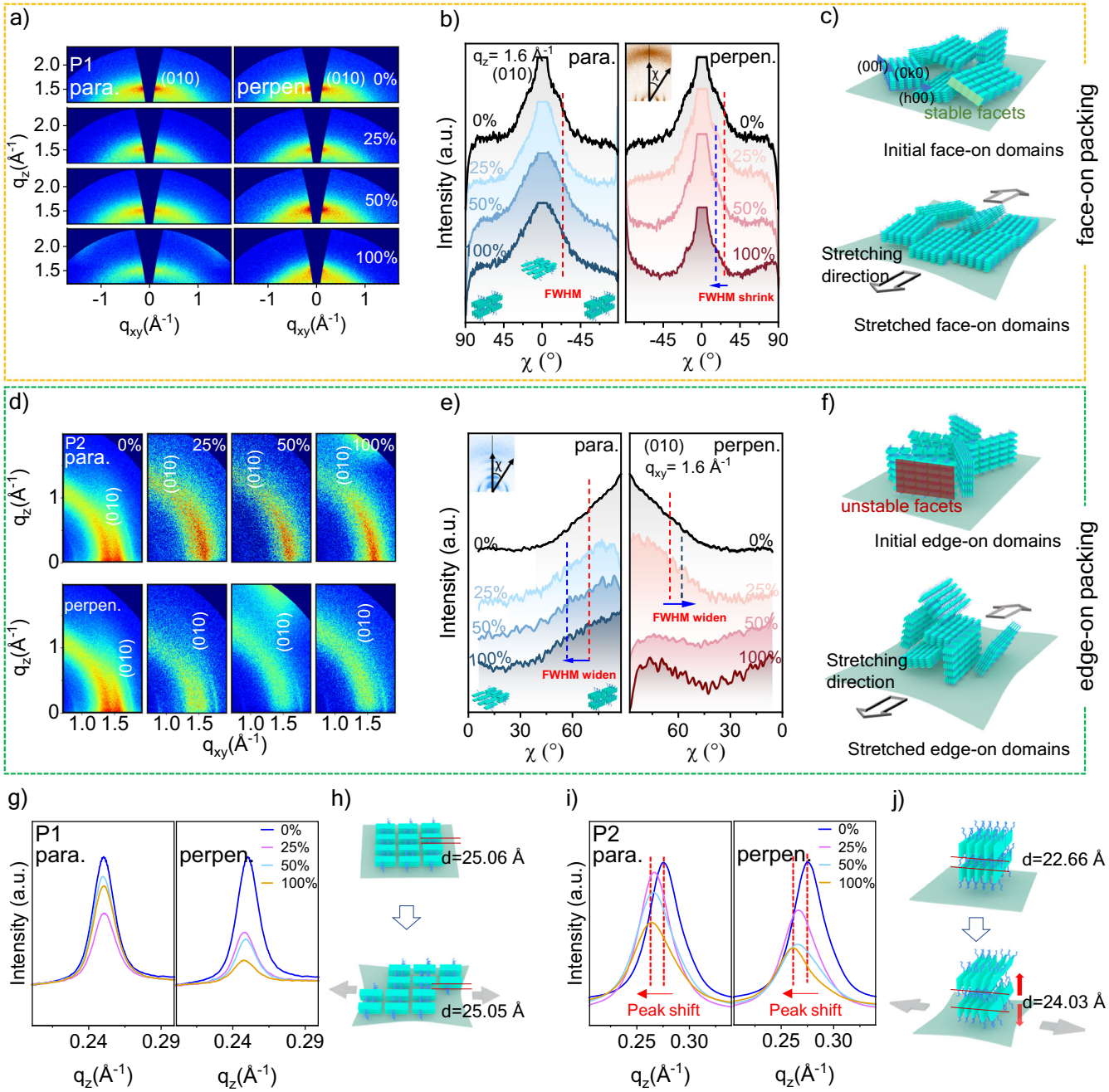

Fig. 4 Strain-induced crystal rotation in conjugated polymer films and the dynamic packing ordering. a, **d** 2D GIWAXS patterns of P1 and P2, (**b**, **e**) Peak intensity of (010) peak as a function of azimuth angle. **c**, **f** Schematic of the morphological evolution of face-on- and edge-on-packed domains under strain. **g**, **i** (100) profiles extracted from the 2D GIWAXS patterns. **h**, **j** Illustration of lamellae packing distance during stretching in face-on and edge-on aggregates.

Crystalline domains in the semiconducting polymer films were observed to align in the substrate plane and rotate out-of-plane to dissipate the strain energy. During this process, the more promising face-on-packed aggregates exhibited enhanced spatial ordering via polymer chains alignment and reorientated backbone π-π stacking. In contrast, the in-plane alignment and out-of-plane rotation of the edge-on-packed aggregates made opposite contributions to the structural ordering. As shown in this study, the rotation of a mass of crystalline domains severely distorts the π-π stacking orientation of polymer backbones. Furthermore, strain increases the lamellae packing disorder in edge-on aggregates. In the coming section, using the UV-DRS characterization, we will clarify the underlying correlation between the different morphological evolution and electrical performance in face-on/edge-on aggregates.

Orientation-dependent energetic disorder evolution under strain

Having a picture of the strain-induced structural evolution in the sub-aggregate scale, we attempted to verify the impact of morphology on the electrical performance by evaluating the degree of energetic disorder in the investigated films. Dependent on the microstructure of the semiconducting materials, the energetic disorder is a crucial factor that determines degradation of charge transport. Configuration disorder at multiple scale

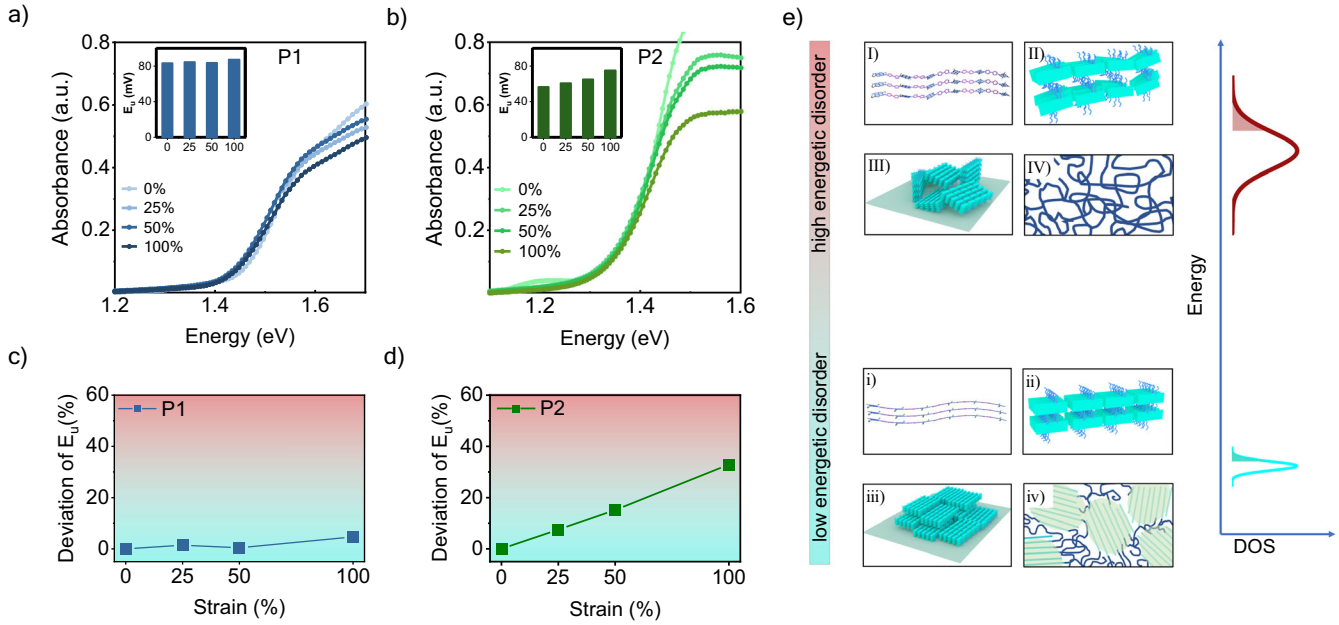

Fig. 5 Energetic disorder in the investigated films under strain. a, **b** Absorbance determined via UV-DRS measurements (insert: Urbach energies of the investigated films). **c**, **d** Deviation in the E_u values of P1 and P2 with increasing strain. **e** Probable structural factors at multiscale contributing to the energetic disorder in stretchable semiconducting polymer films. DOS density of state.

(polymer backbone torsion, lamellae dislocation, crystalline domains orientation and the degree of crystallinity) broaden the electronic density of states (DOS) in semiconducting polymer films (Fig. 5e), dragging tail states further into the bandgap[47–49]. This impedes efficient charge transport by providing additional pathways toward sleep states. In photoactive layers, Urbach energy (E_u) is used to evaluate the degree of energetic disorder (extracted from the optical absorption coefficient in the low photon energy according to the Urbach rule [Supporting information])[47,50]. For semiconducting polymer films prepared using the same material, a higher E_u corresponds to a greater energetic disorder and, accordingly, a larger degradation in charge transport.

UV-vis-DRS was performed on the stretched polymer films to access the E_u of the stretched semiconducting films. The details of the E_u values of P1 and P2 are presented in Supplementary Table 4. P1 has an E_u of 83.3 m eV (Fig. 5a), quite close to the previously reported value[47]. And P2 shows a slightly lower E_u of 56.5 m eV, corresponding to the more efficient charge transport than P1 in rigid OFETs (Supplementary Figs. 6, 7). This is readily comprehensible because when the polymer films are cast from α-CN solution, both the weak backbone aggregation and slower film drying process ensure the polymer chains more stable and ordered structure. When applied to increasing strain, E_u in both types of films exhibit a clearly linear correlation to the strain, suggesting a convincing correlation between strain-induced morphological evolution and energetic disorder in stretchable semiconducting polymer films. Upon stretching to 100% strain, the P1 semiconducting polymer films demonstrated an increment of only 13% in E_u (from 83.26 m eV to 87.26 m eV), whereas the E_u of P2 reached up to 133% when twofold stretched. Considering the inherent energetic disorder originating from polymer chains torsion and elongation for dissipating strain energy[51], the small increase of E_u confirms the promoted ordering of crystalline domains in the face-on-packed films, indicating a well-reserved electronic structure within the films. In contrast, largely strain-induced expanding E_u in edge-on packing N2200 films can be well interpreted by the strain-induced π-π stacking disorder of polymer backbones and lamellae dislocation, as proved by the GIWAXS characterization (Fig. 5e). These results consistently confirm that packing orientation of backbones has a huge impact on the energetic disorder in stretched semiconducting polymer films and the face-on-packed films demonstrate strain-insensitive energetic disorder, promising efficient charge transport under large strain.

For semiconducting polymer films, high mobility counts on the high-level ordering of aggregates, as the charge transport occurs mainly along the backbones of the polymer chains, as well as inter-chains via hopping through the π-π conjugation. Here we assumed that the charge transport in our stretchable OFETs can be described as three-dimensional model, for the bottom gate device structure and relative low mobility[52]. By this model, the complex morphological evolution in the bulk has subtle impacts on the charge transport through the polymer films. Combined with the GIWAXS and UV-DRS characterizations, we elucidated the structural origin of the distinguishing electrical performance in stretched face-on-/edge-on-packed films. The strain facilitates the 3D packing ordering of the face-on-packed aggregates, leading to a strain-insensitive energetic disorder. This morphological evolution enhanced three-dimensional charge transport in the face-on aggregates. Strain-enhanced mobility by quelling the structural disorder in molecular crystals was also reported before[53,54]. Takeya's group have revealed that the suppressed molecular vibrations under compression strain enabled enhanced charge transfer in small molecular crystals (Supplementary Table 6). Considering the structural heterogeneity of conjugated polymers, we investigated the structural origin of energetic disorder from the perspective of aggregates. GIWAXS results revealed that crystallite in-plane alignment and out-of-plane rotation under stretching strain. The resultant energetic disorder was visualized by the Urbach energy. Moreover, our work figured out the structural origin of the dynamic disorder in response to strain on the aggregate scale. By this mechanism, an opposite impact on the edge-on packed aggregates was also interpreted. For the edge-on aggregates, multiple strain-induced disorders within the crystalline domains override the merit of the polymer chains alignment in the substrate plane, as verified by the largely expanding energetic disorder in UV-DRS results. This morphological damage impedes spatial charge transport in edge-on-packed films, thereby resulting in a straight declining electrical

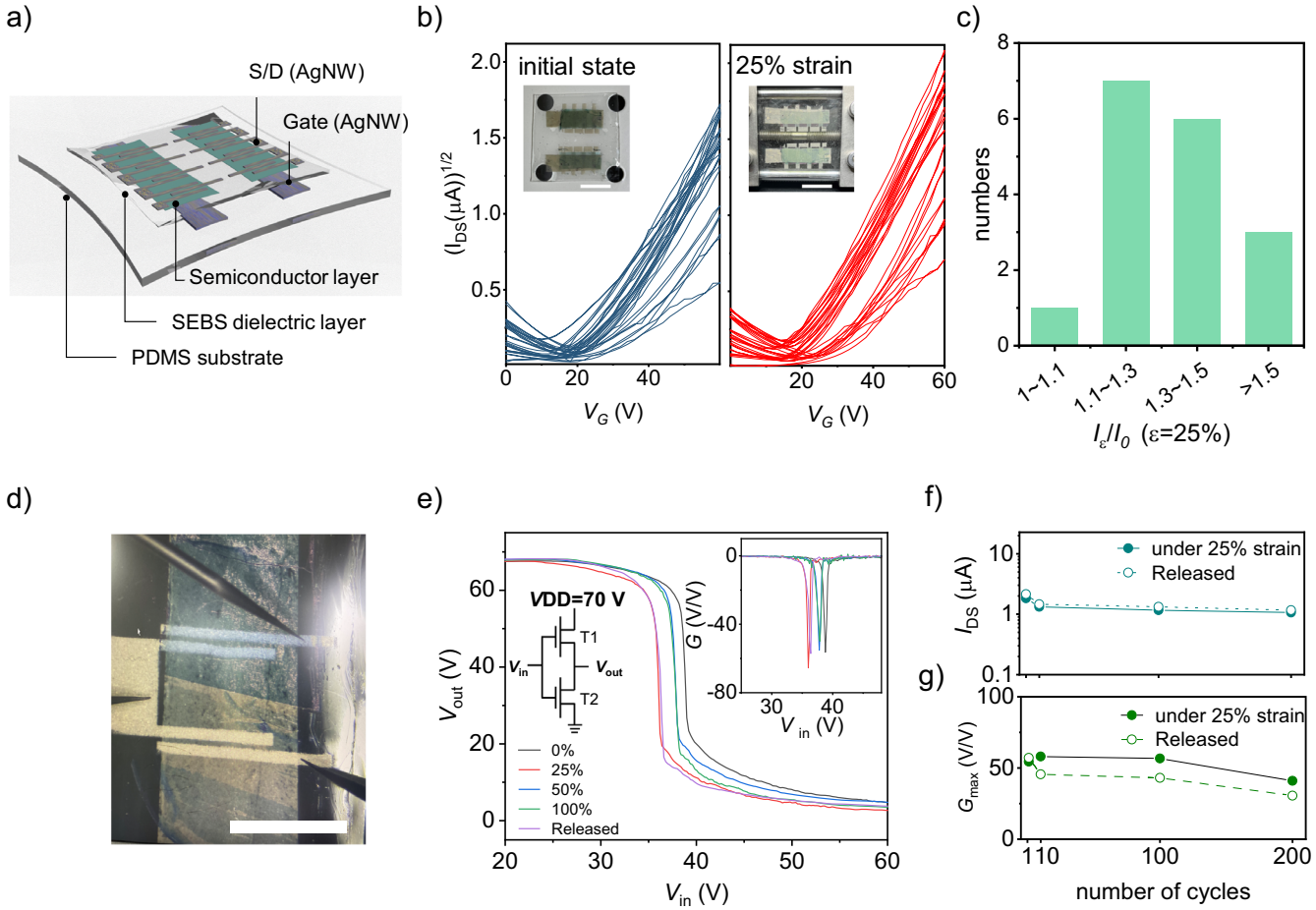

Fig. 6 Stretchable organic transistor array and inverter based on face-on-packed N2200 films. a Schematic of the stretchable organic transistor array. Polydimethylsiloxane, styrene-ethylene-butylene-styrene and Ag nanowire serve as stretchable substrate, stretchable dielectric layer and stretchable electrodes, respectively. **b** On-current before(left) and after (right) stretching to 25% in 16 devices with varying channel widths (from about 3000 μm to 5000 μm). Insert: the stretchable organic transistors array before and after stretching. Scale bar, 10 mm. **c** The statistical distribution of I_ε/I_0. **d** An optical image of a real device with the face-on-packed N2200 films as active layers. Scale bar, 5 mm. **e** The output and gain curves (insert) under various strains. Performance of (**f**) stretchable OFETs and (**g**) inverters under repeating cycles.

performance in stretchable OFETs. This finding helps to explain the degradation of electrical performance of stretched semiconducting polymer films with high degree of chains alignment and no visible cracks generating. For example, the stretchability of a group of edge-on packed DPP-based polymers were studied by Gu's group[34], in which a remarkable polymer chains alignment along the stretching direction was observed via various X-ray characterizations and no cracks generated over the entire investigating range. Nevertheless, all the stretchable OFETs in that work did not maintain effective charge transport under strain. In this case, it is reasonable to infer that strain-induced disordered π-π stacking in the DPP polymer films overrides the merit of chains alignment, which resulted in damaged charge transport in OFETs. Overall, these results emphasize that the orientation of semiconducting polymer backbone has a vital impact on the electrical property of semiconducting polymer films under strain and the face-on-packed aggregates show a higher stability against stretching deformation.

Stretchable organic transistor array and inverter

To demonstrate the superiority of the face-on-packed conjugated polymer films in the application of stretchable organic circuit, a fully stretchable organic transistors array and a complementary inverter were fabricated, using the face-on-packed N2200 films[7]. Figure 6a shows the configuration of the organic transistor array with a bottom-gate top-contact structure. The square roots of the on-current of 16 transistors with varying channel-length/width ratios in the initial state before and after stretching to 25% were compared (Fig. 6c). A statistically significant increment of on-current is observed after stretching. Accordingly, the statistical distribution of I_ε/I_0 (strain = 25%; Fig. 6c) shows that the strain-induced enhancement of on-current mainly occurs between 10% and 50%. Figure 6d shows an optical microscope of the stretchable organic inverter at work, where the organic transistors based on face-on packed N2200 function in n-type and p-type at conditioned voltages, respectively. The fabrication of stretchable organic complementary inverter and work mechanism are detailed in the supporting information (Supplementary Fig. 16). When applied to various strains, the stretchable inverter exhibits similar gains (55–65; Fig. 6e). In addition to the enhancement of the charge carrier transport with a strain of 25%, the gain also shows an increment from 55 (initial state) to 65. To the best of our knowledge, this is the highest value in a stretchable organic pseudo-CMOS inverter simply fabricated by one layer of one-component semiconducting polymer[1,3,17,37]. This proof-of-concept device with a strain-resistant performance provides a strategy to simplify the design of stretchable organic circuits. Finally, we stretched these OFETs up to 200 recycles to investigate the stability and robustness of the targeted OFETs. Both the organic transistors and the complementary inverter

demonstrate robust electrical performance after repeating stretching (Fig. 6f, g and Supplementary Figs. 17, 18), indicating the potential of this face-on-packed polymer films for futural stretchable electronics.

We demonstrate that molecular orientation has an evident impact on the morphological evolution and electrical performance of the stretched conjugated polymer films; and robust electrical performance under strain can be realized by quelling the microstructural disorders within the face-on packed aggregates. Compared to initial state, stretched OFETs based on face-on-oriented N2200 films exhibited a 1.5× increase in on-current and 2× increase in mobility, in sharp contrast to the straight decline in the edge-on cases. Combining morphological and photoelectric characterizations, we directly observed two types of aggregates motion to dissipate the strain energy: (1) polymer chains alignment along the strain; (2) out-of-plane rotation toward the substrate. These motions facilitated the spatial ordering in face-on aggregations and led to strain-insensitive energetic disorder in conjugated polymer films, enabling enhanced three-dimensional charge transport. In contrast, the rotation of the crystalline domains significantly distorted the structural ordering of the edge-on aggregates and increased the energetic disorder in the conjugated polymer films, impeding efficient inter-chain charge transport. In brief, polymer films with face-on orientation exhibited superior stability against stretching deformation due to the strain-induced 3D ordering of aggregations. These findings deepen our understanding of the underlying correlation between the morphological evolution and electrical performance of stretchable semiconducting polymers. Moreover, they provide guidance for designing and processing high-performance semiconducting films for stretchable electronics.

METHODS

Fabrication of the stretchable organic field transistors

We used the PDMS substrate to pick up the upper layers with the order of the gate electrode, dielectric layer, the OSC layer and finally the source and drain electrodes. Finally, the stretchable organic field transistors were fabricated. Here, the channel length and width are 100 and 3000–5000 μm, respectively.

Morphology characterization

Conjugated thin films were laminated by the stretchable substrate and stretched. For the GIWAXS, AFM and UV-DRS characterization, the whole sample was pasted back to the silicon wafer or quartz plate for measurements. Optical images of the films were taken with an optical microscope (Nikon LV100ND). The AFM images were performed with a non-contact mode using a Multimode 8 (Bruker). UV-vis spectra were measured by a UV-2600 (Shimadzu) to measure the absorption intensity with the polarization parallel and perpendicular to the stretching directions. GIXRD images were collected in ambient conditions at the Shanghai Synchrotron Radiation Facility. The incidence angle of the X-ray was 0.334°. Numerical integration of the diffraction peak areas was performed using Dioptas and Fit2d.

UV-vis diffuse reflection spectroscopy

UV-vis diffuse reflection spectra were measured by a UV-2600 (Shimadzu). Films were stretched to 0–100% strain and pasted to the quartz plate for the UV-DRS characterization with a waveband ranging from 200 nm to 1200 nm. Urbach energy is extracted from the exponential fitted absorbance curve according to the formula:

$$\text{Absorbance} \propto e^{\frac{E}{E_u}} \quad (1)$$

where the E is the photo energy and E_u is the Urbach energy.

DATA AVAILABILITY

The data that support the findings of this study are available from the corresponding author upon reasonable request.

Received: 13 March 2023; Accepted: 23 July 2023;
Published online: 01 August 2023

REFERENCES

1. Jager, E. W. H., Smela, E. & Inganas, O. Microfabricating conjugated polymer actuators. *Science* **290**, 1540–1545 (2000).
2. Wang, S. et al. Skin electronics from scalable fabrication of an intrinsically stretchable transistor array. *Nature* **555**, 83–88 (2018).
3. Xu, J. et al. Tuning Conjugated Polymer Chain Packing for Stretchable Semiconductors. *Adv. Mater.* **34**, 2104747 (2022).
4. Zhang, Z. T. et al. Conjugated Polymers for Flexible Energy Harvesting and Storage. *Adv. Mater.* **30**, 1704261 (2018).
5. Yu, X. et al. Incorporation of hydrogen-bonding units into polymeric semiconductors toward boosting charge mobility, intrinsic stretchability, and self-healing ability. *SmartMat* **2**, 347–366 (2021).
6. Gu, P. C. et al. High performance organic transistors and phototransistors based on diketopyrrolopyrrole-quaterthiophene copolymer thin films fabricated via low-concentration solution processing. *Chin. Chem. Lett.* **29**, 1675–1680 (2018).
7. Zhao, Y. et al. All-solution-processed, high-performance n-channel organic transistors and circuits: toward low-cost ambient electronics. *Adv. Mater.* **23**, 2448–2453 (2011).
8. Yan, Y. et al. An OFET-Based Involutive Logic Circuit with Wide-Range Threshold Shift Compensability. *Adv. Electron. Mater.* **8**, 2200442 (2022).
9. Lin, Y.-C., Yang, W.-C., Chiang, Y.-C. & Chen, W.-C. Recent Advances in Organic Phototransistors: Nonvolatile Memory, Artificial Synapses, and Photodetectors. *Small Sci.* **2**, 2100109 (2022).
10. Chen, Q., Zhao, Y. & Liu, Y. Current development in wearable glucose meters. *Chin. Chem. Lett.* **32**, 3705–3717 (2021).
11. Roth, B. et al. Mechanical Properties of a Library of Low-Band-Gap Polymers. *Chem. Mater.* **28**, 2363–2373 (2016).
12. Wu, H. C. et al. A Rapid and Facile Soft Contact Lamination Method: Evaluation of Polymer Semiconductors for Stretchable Transistors. *Chem. Mater.* **26**, 4544–4551 (2014).
13. Zhao, Y. et al. Continuous Melt-Drawing of Highly Aligned Flexible and Stretchable Semiconducting Microfibers for Organic Electronics. *Adv. Funct. Mater.* **28**, 1705584 (2018).
14. Chen, J. et al. Highly stretchable organic electrochemical transistors with strain-resistant performance. *Nat. Mater.* **21**, 564–571 (2022).
15. Lin, Y. C. et al. Study on Intrinsic Stretchability of Diketopyrrolopyrrole-Based π-Conjugated Copolymers with Poly(acryl amide) Side Chains for Organic Field-Effect Transistors. *ACS Appl. Mater. Interfac.* **12**, 33014–33027 (2020).
16. Lu, C. et al. Effects of Molecular Structure and Packing Order on the Stretchability of Semicrystalline Conjugated Poly(Tetrathienoacene-diketopyrrolopyrrole) Polymers. *Adv. Electron. Mater.* **3**, 1600311 (2017).
17. Dai, Y., Hu, H., Wang, M., Xu, J. & Wang, S. Stretchable transistors and functional circuits for human-integrated electronics. *Nat. Electron.* **4**, 17–29 (2021).
18. Printz, A. D. & Lipomi, D. J. Competition between deformability and charge transport in semiconducting polymers for flexible and stretchable electronics. *Appl. Phys. Rev.* **3**, 021302 (2016).
19. Rivnay, J., Mannsfeld, S. C. B., Miller, C. E., Salleo, A. & Toney, M. F. Quantitative determination of organic semiconductor microstructure from the molecular to device scale. *Chem. Rev.* **112**, 5488–5519 (2012).
20. Rivnay, J. et al. Drastic control of texture in a high performance n-type polymeric semiconductor and implications for charge transport. *Macromolecules* **44**, 5246–5255 (2011).
21. Noriega, R. et al. A general relationship between disorder, aggregation and charge transport in conjugated polymers. *Nat. Mater.* **12**, 1038–1044 (2013).
22. Osaka, I. & Takimiya, K. Backbone orientation in semiconducting polymers. *Polymer* **59**, A1–A15 (2015).
23. Sirringhaus, H. et al. Two-dimensional charge transport in self-organized, high-mobility conjugated polymers. *Nature* **401**, 685–688 (1999).
24. Guo, X., Puniredd, S. R., Baumgarten, M., Pisula, W. & Müllen, K. Rational design of benzotrithiophene-diketopyrrolopyrrole-containing donor-acceptor polymers for improved charge carrier transport. *Adv. Mater.* **25**, 5467–5472 (2013).
25. Chen, D., Nakahara, A., Wei, D., Nordlund, D. & Russell, T. P. P3HT/PCBM bulk heterojunction organic photovoltaics: Correlating efficiency and morphology. *Nano Lett.* **11**, 561–567 (2011).

26. Sirringhaus, H., Tessler, N. & Friend, R. H. Integrated optoelectronic devices based on conjugated polymers. *Science* **280**, 1741–1744 (1998).
27. Osaka, I., Kakara, T., Takemura, N., Koganezawa, T. & Takimiya, K. Naphthodithiophene-naphthobisthiadiazole copolymers for solar cells: Alkylation drives the polymer backbone flat and promotes efficiency. *J. Am. Chem. Soc.* **135**, 8834–8837 (2013).
28. Osaka, I., Saito, M., Koganezawa, T. & Takimiya, K. Thiophene-thiazolothiazole copolymers: Significant impact of side chain composition on backbone orientation and solar cell performances. *Adv. Mater.* **26**, 331–338 (2014).
29. Mun, J. W. et al. Effect of Nonconjugated Spacers on Mechanical Properties of Semiconducting Polymers for Stretchable Transistors. *Adv. Funct. Mater.* **28**, 1804222 (2018).
30. Zhao, Y. et al. Melt-Processing of Complementary Semiconducting Polymer Blends for High Performance Organic Transistors. *Adv. Mater.* **29**, 1605056 (2017).
31. Dai, Y. et al. Stretchable Redox-Active Semiconducting Polymers for High-Performance Organic Electrochemical Transistors. *Adv. Mater.* **34**, 2201178 (2022).
32. Wu, H. C. et al. Metal-Ligand Based Mechanophores Enhance Both Mechanical Robustness and Electronic Performance of Polymer Semiconductors. *Adv. Funct. Mater.* **31**, 2009201 (2021).
33. Zheng, Y. et al. Tuning the Mechanical Properties of a Polymer Semiconductor by Modulating Hydrogen Bonding Interactions. *Chem. Mater.* **32**, 5700–5714 (2020).
34. Zhang, S. et al. Molecular Origin of Strain-Induced Chain Alignment in PDPP-Based Semiconducting Polymeric Thin Films. *Adv. Funct. Mater.* **31**, 202100161 (2021).
35. Zhang, S. et al. Toward the Prediction and Control of Glass Transition Temperature for Donor-Acceptor Polymers. *Adv. Funct. Mater.* **30**, 2002221 (2020).
36. Xu, J. et al. Highly stretchable polymer semiconductor films through the nanoconfinement effect. *Science* **355**, 59–64 (2017).
37. Guan, Y.-S. et al. Elastic electronics based on micromesh-structured rubbery semiconductor films. *Nat. Electron.* **5**, 881–892 (2022).
38. Mun, J. et al. F4-TCNQ as an Additive to Impart Stretchable Semiconductors with High Mobility and Stability. *Adv. Electron. Mater.* **6**, 2000251 (2020).
39. Zhou, K. et al. Molecular Orientation of Polymer Acceptor Dominates Open-Circuit Voltage Losses in All-Polymer Solar Cells. *ACS Energy Lett.* **4**, 1057–1064 (2019).
40. Diao, Y. et al. Flow-enhanced solution printing of all-polymer solar cells. *Nat. Commun.* **6**, 7955 (2015).
41. Zhang, F., Mohammadi, E., Qu, G., Dai, X. & Diao, Y. Orientation-Dependent Host-Dopant Interactions for Manipulating Charge Transport in Conjugated Polymers. *Adv. Mater.* **32**, 2002823 (2020).
42. Zhang, S. et al. Directly Probing the Fracture Behavior of Ultrathin Polymeric Films. *ACS Polym. Au.* **1**, 16–29 (2021).
43. Sadler, D. M. New explanation for chain folding in polymers. *Nature* **326**, 174–177 (1987).
44. Yang, L. et al. Molecular Packing and Charge Transport Behaviors of Semiconducting Polymers Over a Wide Temperature Range. *Adv. Funct. Mater.* **32**, 2202456 (2022).
45. Persson, N. E., Engmann, S., Richter, L. J. & DeLongchamp, D. M. In Situ Observation of Alignment Templating by Seed Crystals in Highly Anisotropic Polymer Transistors. *Chem. Mater.* **31**, 4133–4147 (2019).
46. O'Connor, B. et al. Anisotropic Structure and Charge Transport in Highly Strain-Aligned Regioregular Poly(3-hexylthiophene). *Adv. Funct. Mater.* **21**, 3697–3705 (2011).
47. Kronemeijer, A. J. et al. Two-dimensional carrier distribution in top-gate polymer field-effect transistors: Correlation between width of density of localized states and urbach energy. *Adv. Mater.* **26**, 728–733 (2014).
48. Schweicher, G. et al. Chasing the "Killer" Phonon Mode for the Rational Design of Low-Disorder, High-Mobility Molecular Semiconductors. *Adv. Mater.* **31**, 1902407 (2019).
49. Venkateshvaran, D. et al. Approaching disorder-free transport in high-mobility conjugated polymers. *Nature* **515**, 384–388 (2014).
50. Liu, S. et al. High-efficiency organic solar cells with low non-radiative recombination loss and low energetic disorder. *Nat. Photon.* **14**, 300–305 (2020).
51. Zheng, Y., Zhang, S., Tok, J. B. H. & Bao, Z. Molecular Design of Stretchable Polymer Semiconductors: Current Progress and Future Directions. *J. Am. Chem. Soc.* **144**, 4699–4715 (2022).
52. Brondijk, J. J. et al. Two-dimensional charge transport in disordered organic semiconductors. *Phys. Rev. Lett.* **109**, 056601 (2012).
53. Kubo, T. et al. Suppressing molecular vibrations in organic semiconductors by inducing strain. *Nat. Commun.* **7**, 11156 (2016).
54. Sakai, K. et al. The emergence of charge coherence in soft molecular organic semiconductors via the suppression of thermal fluctuations. *NPG Asia Mater.* **8**, e252 (2016).

ACKNOWLEDGEMENTS

This research was financially supported by the National Key R&D Program of China (No. 2018YFA0703200), the National Natural Science Foundation of China (Grant Nos. 61890940), and the Natural Science Foundation of Shanghai (22ZR1407800). The authors gratefully acknowledge the Shanghai Synchrotron Radiation Facility (SSRF) for providing the precious time and the Synchrotron XRD Facility at Beamline NO. 14B/15U.

AUTHOR CONTRIBUTIONS

Q.Z. and Y.Z. conceived the idea and designed the experiment. Y.L. supervised the project. Q.Z. and Z.W. fabricated the stretchable OFETs. Q.Z. performed all the experiments for material- and devices characterization, and analyzed all the experimental data. Q.Z. wrote the whole paper. Y.Z. reviewed the paper. All the authors gave valuable comments on this paper.

COMPETING INTERESTS

The authors declare no competing interests.

ADDITIONAL INFORMATION

Supplementary information The online version contains supplementary material available at https://doi.org/10.1038/s41528-023-00269-w.

Correspondence and requests for materials should be addressed to Yan Zhao.

Reprints and permission information is available at http://www.nature.com/reprints

Publisher's note Springer Nature remains neutral with regard to jurisdictional claims in published maps and institutional affiliations.